AN ABSTRACT OF THE THESIS OF

Priscilla Newberger for the Doctor of Philosophy

in Oceanography presented on August 4, 1980

Title: Turbulence in the Bottom Boundary Layer

Redacted for privacy

Abstract approved:

D. R. Caldwell

Vertical profiles of temperature, temperature-gradient and, in some cases, light transmissivity are used to examine the turbulence in the bottom boundary layer on the Oregon shelf. Two data sets are studied. The first, discussed in Chapter I, is used to test the hypothesis that the bottom layer is a turbulent boundary layer with the distribution of heat and suspended sediment determined by the turbulent transport of these quantities. Vertical temperature-gradient spectra from the second are analysed in Chapter II. The ensemble average of these spectra is compared with the predicted universal form. The inertial range as well as the Batchelor range is observed.

A close relationship between active mixing and the structure of the bottom nepheloid layer is shown in Chapter I. Mechanical-energy dissipation rates and eddy coefficients are usually consistent with those in an unstratified turbulent boundary layer, but an

exception was found when stratification due to suspended sediment was required to explain the observations. Except in this case, the suspended particle concentration, for observations in approximately 100 m of water, are consistent with the assumption of local equilibrium between turbulent diffusion and gravitational settling. Observations made in deeper (180 to 200 m) water do not show this balance.

The high gradient region above the nepheloid layer in shallow water impedes diffusion sufficiently that escape of particles by this route is not important. The region of low turbulent mixing was not consistently seen in deeper water where high levels of turbidity were found throughout the water column. Low-density turbidity currents of approximately 1 cm s^{-1} can be generated by the suspended sediment concentrations found.

An inertial subrange was found in spectra calculated in Chapter II. Spectra were calculated for each 53 cm vertical segment of the bottom layer. An ensemble average of those spectra that were fully resolved and had high Cox number was compared to the universal form. Good agreement was found with the Batchelor form. The high wavenumber end of the inertial range was resolved. A relationship between the Kolmogorov constant for temperature, β, and the Batchelor constant, q, was established, $\beta q^{-2/3} = 0.172$. If $\beta = 0.5$, as determined from atmospheric measurements, $q = 4.95$ $(4.29 < q < 6.65)$ and the transition from the inertial to the viscous-convective range occurs at a wavenumber $k = 0.035\ k_K$ $(0.021 < k/k_K < 0.043)$ where k_K is the Kolmogorov wavenumber.

Turbulence in the Bottom Boundary Layer

by

Priscilla Anne Newberger

A THESIS

submitted to

Oregon State University

in partial fulfillment of
the requirements for the
degree of

Doctor of Philosophy

June 1981

APPROVED:

Redacted for privacy

Professor of Oceanography
in charge of major

Redacted for privacy

Associate Dean of Oceanography

Redacted for privacy

Dean of Graduate School

Date thesis is presented August 4, 1980

Typed by Pam Wegner for Priscilla Newberger

ACKNOWLEDGMENTS

I thank my major professor, Dr. D. R. Caldwell for his help, insight and patience.

Many students and staff of the School of Oceanography have helped with the data collection. I thank them all. Steve Wilcox, Mark Matsler, Stuart Blood, Terry Chriss, John Brubaker and Stuart Eide have each contributed significant skill and effort. Dr. Tom Dillon acted as major professor during Dr. Caldwell's absence. I also thank my committee.

I also thank my family, Stuart and Florence, for their support.

This research was supported by NSF Grants OCE77-20242 and OCE79-18904.

TABLE OF CONTENTS

LIST OF ILLUSTRATIONS

Mixing and the Bottom Nepheloid Layer

P. A. Newberger

School of Oceanography

Oregon State University

Corvallis, Oregon 97331

USA

February 1980

ABSTRACT

A close relationship between active mixing and the structure of the bottom nepheloid layer on the Oregon shelf is shown, by combining mixing information inferred from temperature microstructure with concentration profiles derived from a transmissometer mounted on the microstructure instrument. Mechanical energy dissipation rates and eddy coefficients are usually consistent with those in an unstratified turbulent boundary layer, but an exception was found when stratification due to suspended sediment was required to explain the observations. Except for this case, the suspended particle concentration profiles, for observations in approximately 100 m of water, are consistent with the assumption of local equilibrium between turbulent diffusion and gravitational settling. Observations made in deeper (180 to 200 m) water do not show this balance.

The high gradient region above the nepheloid layer in shallow water impedes diffusion sufficiently that escape of particles by this route is not important; winter mixing destroys the layer long before diffusion would. This region of low turbulent mixing was not consistently seen in the deeper water where high levels of turbidity were found throughout the water column. Low-density turbidity currents of approximately 1 cm s^{-1} can be generated by the concentrations found.

INTRODUCTION

Two prominent features have frequently been observed in the near bottom region on the Oregon shelf, a "mixed" layer approximately 10 m thick with temperature variations of less than 0.003°C (Caldwell, 1976, 1978) and a "nepheloid" layer of increased particle concentration (Komar, Kulm and Harlett, 1974; Pak and Zaneveld, 1977). The relationship between these features has not been understood. Do they occur independently? Is either always present? What process limits the vertical extent, and is it the same for both? Do the same processes control the vertical distribution of suspended particles and heat?

Answering the first two of these questions requires extensive surveying of the area. Some information is available. Komar, Kulm and Harlett (1974) note that the nepheloid layer is thicker in swales, and suggest that gravitationally driven flow of turbid water may be important. Pak and Zaneveld (1977) found a bottom nepheloid layer at least as frequently as a bottom mixed layer. Both were found with increased frequency during periods unfavorable to upwelling.

To determine whether the last two questions can be answered in terms of vertical processes alone, we test the applicability of a model involving vertical turbulent mixing of heat and particles as well as gravitational settling of the particles. We hypothesize that the bottom layer can be described as a turbulent boundary layer containing a near-bottom constant-stress sublayer. This layer is assumed to be capped by a sharp density gradient through

which transport of heat and mass is inhibited. Within the boundary layer, stratification is usually negligible, and classical turbulent boundary layer results apply. The vertical distribution of particles is determined by gravitational settling through the turbulent water.

The data used to evaluate this hypothesis are of three kinds:
(1) Vertical mixing information calculated from profiles of the smallest-scale vertical temperature gradients, measured by a freely falling "microstructure" instrument. This information is presented as eddy-mixing coefficients or kinetic-energy dissipation rates.
(2) Vertical profiles of optical transmissivity from which concentration of total suspended matter is estimated. The transmissometer is mounted on the microstructure instrument.
(3) Horizontal currents measured in or above the layer by nearby moored instruments.

MEASUREMENTS

The temperature microstructure instrument is similar to one previously described in detail (Caldwell, Wilcox and Matsler, 1975), with the addition of a transmissometer. The transmissometer's output is proportional to the light received over a 0.25 m sea water path. The (LED) light source emits light with wavelength 660 nm. This light is not significantly attenuated by dissolved organic substances so that attenuation is caused solely by suspended particles and the water itself (Jerlov, 1968). Temperature sensitivity can be a problem with transmissometers. This transmissometer

is not temperature compensated but was allowed to come to equilibrium with bottom layer temperature before sampling began. Temperature dependence varied among the three units used, with the most sensitive showing a decrease in light received of 0.77% per degree centigrade (temperature variation within a profile was always less than 0.5°C).

The data consist of profiles at two locations along 45°20'N on the Oregon shelf, in 90 to 110 m of water in August and September 1978 and June 1979, and in 180 to 200 m in April and June 1979. Dr. Barbara Hickey of the University of Washington has kindly made available current data from the 1978 sampling periods. Current measurements for 1979 are from bottom-mounted current meters (Caldwell and Chriss, 1979).

Sequences of one to eight profiles through the bottom layer were recorded within a short time, usually less than one hour. As previously observed (Caldwell, 1978) there was considerable variability among the profiles in a sequence; however, mean conditions usually remained sufficiently constant over the sampling interval that each sequence is assumed to consist of several realizations of the same process.

In each of the nine shallow-water sequences there was a near-bottom region of relatively uniform temperature and reduced light transmission (Fig. 1a,b). Only the two from September 1978 differ greatly from the typical form described by Caldwell (1978), which comprises an interface of large vertical temperature-gradient above a layer of nearly uniform temperature. Although the temperature

within the boundary layer is uniform to within a few millidegrees, its upper part is characterized by larger temperature gradients approximately 1 cm thick. Near the bottom there is little of this small scale activity. Caldwell (1978) found the average of the mean temperature gradients to be 1.25 times the adiabatic in the bottom few meters. Small mean gradients of either sign were found in the present data. High levels of mixing as indicated by the Cox number, the ratio of mean square temperature gradient to mean gradient squared, were found throughout the bottom layer.

The thirteen sequences from the deep-water station (approximately 180 m) also show a region of nearly uniform temperature and reduced transmission near the bottom (Fig. 1c,d) but few of these show strong mixing. The interface at the top of the layer is typically less sharp and the overlying water is quite turbid. Only eight of the deep sequences were analysed in detail. Uneven descent rates caused by line tension made the others unsuitable for analysis.

DATA ANALYSIS

Temperature-gradient spectra were calculated from the microstructure records for blocks of 512 points (layers of thickness 0.74 to 1.60 m for the descent rates used) and were corrected for thermistor response (Dillon and Caldwell, 1980). In many cases these spectra resemble the universal forms predicted for fully-developed turbulence (Tennekes and Lumley, 1972) and the high-wavenumber maxima are resolved. In these cases several turbulence

parameters can be estimated directly from the gradient spectra. The rate of dissipation of kinetic energy, ε, can be calculated from the wavenumber of the diffusive cut-off, taken to be the wavenumber at which the spectrum has fallen to 12% of the maximum value (Caldwell et al., 1980). This wavenumber approximates the Batchelor wavenumber:

$$k_{12\%} \simeq k_B = (2\pi)^{-1} (\varepsilon/\nu D^2)^{1/4}$$

where ν is the kinematic viscosity and D the thermal diffusivity. Inversion of this formula allows calculation of ε as $\varepsilon = (2\pi)^4 \nu D^2 k_{12\%}^4$.

Since the high-wavenumber maximum is resolved, the variance of the temperature gradient (corrected for thermistor response) can be obtained by integrating the gradient spectrum. From this the Cox number, which indicates mixing intensity, can be formed:

$$Cox = \langle (dT/dz)^2 \rangle / \langle dT/dz \rangle^2$$

where $\langle\rangle$ denotes an average for a 512 point block. An eddy-coefficient for heat can be calculated with the further assumption that production and dissipation of temperature variance locally balance (Osborn and Cox, 1972):

$$K_H = D \cdot Cox.$$

This estimate cannot be made if the mean gradient over one data block is too small to resolve.

This analysis is limited to spectra resembling the universal form. Much of the water column is not actively turbulent at any given time. Even within turbulent patches the signal level may occasionally not be large enough for the high wavenumber peak to

extend above noise, i.e. isothermal turbulence cannot be seen in this way.

Percent transmission per 0.25 meter was calculated by dividing the observed transmission by transmission over an air path, corrected to bottom-layer temperature. The fourth power of this ratio gives percent transmission per meter. The attenuation coefficient c is the absolute value of the natural logarithm of this number. The beam attenuation depends on the number, size and composition of the suspended particles. If the slope of the particle size distribution is constant, the beam attenuation and number of particles will be linearly related provided that scattering efficiency of particles is the same for all size classes (Zaneveld, 1973). According to Peterson (1978) this is the case for lithogenous particles larger than about 2 μm and organic particles larger than about 7 μm. Because the composition and size distribution of suspended material varies greatly, it is not possible for one formula to relate light transmission to the amount of suspended matter, but Peterson (1978) has obtained an empirical relationship between the attenuation coefficient and total suspended matter (TSM in $\mu g \ell^{-1}$) for the Oregon shelf:

$$TSM = (c - 0.42)/0.00064.$$

This was used to estimate the amount of suspended sediment in the nepheloid layer. Peterson estimated an error of at most ± 70 $\mu g \ell^{-1}$ for this relationship.

THE TURBULENT BOUNDARY LAYER

In order to test the hypothesis that the bottom mixed layer is a turbulent boundary layer, it is necessary to look at the consequences of this assumption. Near a solid boundary the velocity profile in a turbulent, horizontally-homogeneous, neutrally-stratified flow is logarithmic (Monin and Yaglom, 1971). The shear, $d\bar{U}/dz$, is equal to u_*/kz where u_* is the friction velocity ($u_* = (\tau/\rho)^{1/2}$ where τ is the bottom stress and ρ the density), k is von Karman's constant, usually taken to be 0.41, and z the distance above the boundary. Production and dissipation of kinetic energy are nearly equal and the turbulent energy equation can be approximated by

$$\varepsilon = u_*^2 \, d\bar{U}/dz = u_*^3/kz.$$

This relationship makes it possible to estimate u_* from the values of ε derived from the temperature-gradient spectra. Average values of u_* for each data sequence are presented in Table 1 (shallow) and Table 2 (deep).

The relationship $\varepsilon = u_*^3/kz$ predicts that the dissipation rate increases as the bottom is approached. This tendency was observed in all sequences. In most cases there are too few estimates within the near-bottom region and too much scatter in the estimates of ε to determine the functional relationship between ε and z. For one profile (79612E2) ε and z are clearly inversely related (Fig. 2). In this case a linear least-squares fit of log ε to log z has a slope of -0.979 with $u_* = 0.16$ cm s^{-1} ($r = 0.914$) in good agreement with the prediction.

The large scatter observed in estimates of ε from data taken a fixed distance above the bed within a short time may be attributed to the intermittence of boundary layer turbulence. Intermittence of Reynolds stress has been observed in the laboratory (Grass, 1971) and in the field (Heathershaw, 1974; Gordon, 1974; Heathershaw and Simpson, 1978). This variability will also appear in measurements of ε. To estimate turbulent parameters in the bottom boundary layer, it is necessary to sample a representative range and number of events. The average u_* calculated for each sequence includes all estimates of ε within the bottom layer. If this sample is representative, ρu_*^2 is the average bed stress during the sampling period and can be compared to stress estimates made from the current-meter data using the logarithmic-layer relationships.

The velocity profile in the logarithmic region is often given as

$$U(z) = u_* \ln(z/z_o)/k$$

where z_o is the roughness length defined by $U(z_o) = 0$ (Tennekes and Lumley, 1972). This formulation is not appropriate for hydrodynamically smooth flow in which a viscous sublayer with velocity gradient $dU/dz = u_*^2/\nu$ underlies the logarithmic layer. In this case $U(z)$ can be written in terms of δ, the thickness of the viscous sublayer

$$U(z) - U(\delta) = u_* \ln(z/\delta)/k$$

where $U(\delta) = u_*^2\delta/\nu$ is the velocity at the top of the sublayer.

Observations by Chriss and Caldwell (1979) indicate that the flow was hydrodynamically smooth during the April and June 1979

sampling periods. Measurements of u_* and δ in the region of constant velocity gradient just above the sediment made with a profiling heated thermistor predict the velocities measured by the current meter at 59 cm well, indicating that the smooth flow relationships hold. Laboratory studies have shown that δ is approximately equal to 11 ν/u_*. Although the recent work by Chriss and Caldwell (1979) indicates that sublayer thickness is often greater in the ocean, the laboratory results are used to determine friction velocity, u_{*cm}, from the current meter data. Only the data from April and June 1979 were used in this calculation because the current meter 8 m above the bottom is not necessarily within the logarithmic layer.

Values of u_* from microstructure and from the current meter were correlated ($r = 0.755$) for all periods when the 59 cm current meter was above threshold. The microstructure profiles were made within 1 km of the bottom-moored platform. During periods of changing mean current or in the presence of horizontal gradients, it is likely that the two instruments will sample different conditions. Better agreement is expected during periods of steady mean current. For the six microstructure profiles that fall within periods of steady mean current the correlation between the two estimates of u_* is much better ($r = 0.988$). Figure 3 shows ε/u_{*cm}^3 vs. z for these sequences. Assuming the relations mentioned above, we expect ε/u_*^3 to resemble $(kz)^{-1}$. Again the increase as the bottom is approached is evident. The scatter is due at least in part to the intermittency of the turbulence.

With the same assumptions for boundary-layer flow, the eddy

coefficient for momentum, K_M, becomes ku_*z. Assuming that eddy coefficients for heat and momentum are equal, these estimates can be compared with those made directly from the Cox numbers. No Cox number estimates are available for sequences 79612A, 79612C, 79612D and 79420B because the mean temperature gradient was not resolved near the bottom. With one exception (78922A) the value of ku_*z at $z = 100$ cm is within the range of values found near the bottom. It is difficult to form a meaningful average eddy coefficient from the Cox-number estimates because high levels of mixing over patches of small vertical extent contribute relatively little to overall mixing. Estimates of mean eddy coefficients $\bar{K}$ are made by dividing the average variance in the bottom few meters by the mean gradient squared and provide at least a rough approximation (Table 2). Agreement is found between these estimates and ku_*z for the deep drops. Mean gradients were unresolved for too much of the bottom layer to allow estimates of mean eddy coefficient by this method for 79420B, 79607B and all of the shallow drops.

Despite the intermittency of boundary layer processes a consistant picture emerges. Friction velocities inferred from the temperature microstructure are correlated with mean horizontal currents. Eddy coefficients based on friction velocity are within the range of those found directly from temperature-gradient spectra.

THE DISTRIBUTION OF SUSPENDED SEDIMENT

Bassin (1974) states that two factors are necessary for the maintenance of a bottom nepheloid layer. The first is a source of

suspended particles, the second, a layer of nearly molecular diffusivity above the bottom layer which prevents diffusion upward. Periodic resuspension of sediment, settling from above, and advection from the near shore region have been suggested as sources of suspended matter (Komar et al., 1974; Pak and Zaneveld, 1977; Chriss and Pak, 1977). The Cox numbers show the existence of an interface of extremely low diffusivity corresponding to the high transmissivity gradient above the nepheloid layer for all shallow-water sequences (Fig. 1a,b). This interface was typically 1 to 2 m thick with eddy coefficient between 0.002 and 0.004 $cm^2\ s^{-1}$. A mixing time estimate for the destruction of a turbulent bottom layer of thickness H below an interface of thickness h and diffusivity D is $\tau = Hh/D$. For H = 10 m h = 2 m and D = 0.003 $cm^2\ s^{-1}$, τ is approximately two years. On the Oregon shelf the water column is mixed to the bottom during winter storms so that destruction of the bottom nepheloid layer by diffusion does not occur.

In deeper water these conditions do not hold. The low diffusivity layer as indicated by low Cox number is not usually seen at the top of the mixed layer. This water is more turbid than the shallower water and the region of large turbidity-gradient may extend 20 m above the bottom layer (Fig. 1d).

The equation governing the distribution of particles with identical settling velocities in a horizontally-homogeneous turbulent flow is (Taylor and Dyer, 1977)

$$\partial C/\partial t = -\partial J/\partial z = \partial/\partial z(w_s C + K_s\ \partial C/\partial z)$$

where J is the particle flux, C the concentration, w_s the magnitude

of the particle settling velocity, and K_s the eddy coefficient. In the steady case J is equal to $(-w_s C - K_s \partial C/\partial z)$ and does not vary with depth. In the ocean the suspended particles are not uniform in size, density, or composition so that w_s must be taken as an apparent settling velocity.

The assumption of steady state is apparently satisfied for all shallow-water data except the two sequences from September 1978. That is, the amount of suspended sediment in the bottom layer does not vary by more than the uncertainties in the measurements. Large changes in particle concentration during the September 1978 sequences and all those from deep water suggest that horizontal processes may be important and that a simple vertical balance cannot be used.

We will now test the model with shallow-water data which are apparently steady state. There are two simple ways to model K_s. The first assumes that K_s is independent of depth, the second that $K_s = ku_*z$, the eddy coefficient for momentum. We may assume either that the effect of the settling is important or that it may be neglected with respect to turbulent mixing. Combining these assumptions leads to four forms of the equation governing the distribution of particles in the steady flux case. The solutions to the four forms are summarized in Table 3. Each solution predicts a concentration profile to be compared with the observed profiles.

To test these predictions, mean particle concentration profiles were formed for each of the shallow sequences, except those from September 1978. These profiles begin a few centimeters above the

sediment and extend upward approximately 10 m, or to the high-gradient region at the top of the layer. The sequence 79612E was omitted because of spikes in the transmissivity possibly caused by small organisms or large particles passing through the light path.

Each of the remaining seven sequences was fit to the linear forms of the profiles given in Table 3, using a least-squares method. For models III and IV, values of J/w_s from -150 to 150 $\mu g \ell^{-1}$ were tested. In all cases models II and IV gave better fits than models I and III (Fig. 4) indicating that K_s is better modeled by ku_*z. It was not possible to distinguish between models II and IV or between different values of constant flux for model IV on the basis of the fit.

Model II requires an upward flux of particles to maintain the observed near-bottom increase in concentration. The only near-bottom source is provided by resuspension. Currents measured during this period (less than 15 cm s^{-1}) were not nearly large enough to erode the sediment at this location (mixed sand and mud [Runge, 1966]). Thus it is likely that the increase in concentration near the bottom is due to settling of particles through the turbulent water, and therefore that model IV is appropriate.

For constant flux, model IV allows calculation of an apparent settling velocity from the slope of the linear fit (Table 4). These calculated settling velocities can be compared with those computed for the particle sizes and densities found in the nepheloid layer on the Oregon shelf. Minerals of density 2.6 g cm^{-3} make up the bulk of the particles in the layer (Peterson, 1978). A peak in

the particle-diameter distribution between 3 and 7 μm has been observed in samples taken approximately 10 m above the bottom. According to Stokes' law, spheres of this size and density have settling velocities in the range 0.0008 to 0.004 cm s^{-1}, in agreement with the apparent settling velocities calculated from Model IV. The slightly higher values may be due to a shift in the particle size distribution toward larger particles as the bottom is approached.

It is possible to estimate the flux into the bottom layer from above. For June 1979 sequences the concentrations above the nepheloid layer are from 100 to 150 μgℓ^{-1}. In this case the diffusion through the top of the layer is negligible and $-J/w_s$ is approximately equal to the concentration above the layer. This flux would cause an increase in concentration in a 10 m layer of only about 2 μgℓ^{-1} in one hour, much below the resolution of the instrument. In August 1978 concentrations above the nepheloid layer are less than 50 μgℓ^{-1} and the flux is near zero. Assuming no resuspension of sediment, the mean particle-settling velocity, based on a flux from above, is 0.005 cm s^{-1} with standard deviation 0.001.

THE EFFECT ON THE DYNAMICS OF THE BOTTOM LAYER

There are two related processes by which suspended sediment can affect flow dynamics, by introducing a vertical density-gradient within the bottom layer and by causing a gravitationally-driven downslope flow due to the excess density of the turbid water.

Both effects may be important in the anomalous sequences from

September 1978. During this period mean currents eight meters above the bottom were small, less than 5 cm s^{-1} during the first sequence (78921A) and approximately 1 cm s^{-1} during the second (78922A). Large gradients in concentration (implying a buoyancy frequency of 0.5 cph) extended to the bottom. The thermal mixed layer was unusually thin (Fig. 1b). Equilibrium was not found between settling and diffusion of suspended particles. Harlett (1972) suggests that during quiescent periods settling may concentrate enough suspended matter near the bottom to influence the density structure of the layer.

The effect of stratification on turbulent processes has been modeled (Dyer, 1974) by use of a "dimensionless wind" ϕ defined by:

$$\phi \equiv kzu_*^{-1} \, dU/dz.$$

In a stratified flow $\varepsilon = (u_*^3/kz)\phi$ and eddy coefficient $K = ku_*z/\phi$. Combining these relationships,

$$K = (kz/\phi)(kz\varepsilon/\phi)^{1/3}$$

so that the effect of stable stratification ($\phi > 1$) is to reduce the turbulent mixing corresponding to a given dissipation rate ε. In the stable case $\phi = 1 + 5\ z/L$ (Dyer, 1974) where L is the Monin-Obukhov length (Taylor and Dyer, 1977)

$$L \equiv \frac{\rho u_*^3}{kg(\overline{\rho' w'})}$$

where g is gravitational acceleration and ρ' and w' are turbulent fluctuations of density and vertical velocity respectively. With an eddy-coefficient assumption, $(\overline{\rho' w'}) = -K_s \frac{\partial \rho}{\partial z}$ if the density gradient is assumed to be due to the observed suspended-sediment

gradient. If ku_*L/ϕ is the appropriate eddy coefficient, the Monin-Obukhov length and revised estimates of u_* can be calculated iteratively: for sequence 78921A, L = 7.7 m, $u_* = 0.13$ cm s^{-1} and $K = ku_*z/\phi = 3.3$ cm^2 s^{-1} at z = 1 m. This lies within the range of 2-20 cm^2 s^{-1} for the eddy coefficient for heat estimated from the Cox numbers. For 78922A, L = 1.8 m, $u_* = 0.03$ cm s^{-1} and K = 0.3 cm^2 s^{-1} at 1 meter. Here the Cox number estimates range from 0.02 to 0.1 cm^2 s^{-1}. Thus the density gradient due to suspended sediment is sufficient to explain the discrepancies between observations and the predictions based on neutral stratification.

The possibility that low-density turbidity currents flowing across the continental shelf provide significant transport of sediment onto the slope has been discussed by several authors (McCave, 1972; Drake, 1974; Komar et al., 1974). In the absence of cross-shelf density gradients due to temperature or salinity, the velocity due to excess density can be approximated by (Kullenberg, 1974)

$$V = C_d^{-1/2}(Hg(\Delta\rho/\rho)\ \sin\theta)^{1/2},$$

where H is the flow thickness, $\Delta\rho$ the excess density and sin θ the bottom slope. C_d is a drag coefficient taking into account both bottom friction and the drag of overlying water. Kullenberg (1974) gives a range of values $3 \times 10^{-3} \leq C_d \leq 3 \times 10^{-2}$.

Using this approximation and a value of 0.01 for C_d, the velocity was 0.5 cm/s during 78921A and 78922A. Velocities of 2.8 cm/s and 0.4 cm/s respectively were measured 8 m above the sediment. Velocities of up to 1 cm/s are estimated for the more typical

shallow water drops. During periods of small current, suspended sediment may contribute significantly to offshore flow.

CONCLUSIONS

1. The dissipation information is consistent with the model of a classical turbulent boundary layer:

   a) Profiles of dissipation rate ε are consistent with the existence of a layer in which production and dissipation of kinetic energy are nearly equal.

   b) Values of u_* calculated from the ε profiles are correlated with the friction velocity calculated from the mean currents. During long periods of steady mean current this correlation is very good ($r = 0.988$).

   c) Values of $K = k\, u_* z$ are in agreement with eddy coefficients calculated directly from temperature-gradient spectra for all sequences except 78922A. Agreement is found for this sequence and 78921A when the stratification caused by the large suspended-sediment concentration gradient is taken into account.

2. At approximately 100 m depth the suspended-sediment distribution in the boundary layer is explainable by a model balancing gravitational settling and turbulent diffusion except in two cases, sequences 78921A and 78922A. Particles are trapped in the layer by a region of near-molecular diffusivity. At 180 m neither of these statements is true.

   a) Models assuming that the eddy coefficient for suspended sediment is equal to ku_*z fit the 100 m data significantly

better than models assuming mixing independent of depth.

b) It is not possible to distinguish between models neglecting particle settling and those including it on the basis of goodness of fit. The lack of a particle source at the bottom (given the observed currents) suggests that settling is necessary to maintain the near-bottom concentration increase.

c) Assuming that the flux through the layer is determined by settling through the region of near-molecular diffusivity, an apparent particle-settling velocity of 0.005 cm s^{-1} is indicated.

d) In deep water ($\sim$200 m) we do not find local equilibrium. Large changes in turbidity occur within brief periods and a steady, one-dimensional balance cannot explain these profiles.

3. The presence of suspended matter can affect both stability and offshore flow.

a) For sequences 78921A and 78922A the observed concentration gradients imply a buoyancy frequency of 0.5 cph.

b) Contributions to near-bottom cross-shelf velocities of approximately 1 cm s^{-1} are estimated for the 100 m suspended sediment concentrations.

ACKNOWLEDGEMENTS

We thank Dr. Barbara Hickey and Terry Chriss for providing current data. This research was supported by NSF Grant CE77-20242.

REFERENCES

Bassin, N. J., 1974. Suspended matter and stability of the water column, Central Caribbean Sea. In: R. J. Gibbs (Editor), Suspended Solids in Water. Plenum, New York, pp. 195-202.

Caldwell, D. R., 1976. Fine-scale temperature structure in the bottom mixed layer on the Oregon shelf. Deep-Sea Research, 23:1025-1035.

Caldwell, D. R., 1978. Variability of the bottom mixed layer on the Oregon shelf. Deep-Sea Research, 25:1235-1243.

Caldwell, D. R. and Chriss, T. M., 1979. The viscous sublayer at the sea floor. Science, 205:1131-1132.

Caldwell, D. R., Wilcox, S. D. and Matsler, M., 1975. A relatively simple freely falling probe for small-scale temperature gradients. Limnology and Oceanography, 20:1035-1042.

Caldwell, D. R., Dillon, T. M., Brubaker, J. M., Newberger, P. A. and Paulson, C. A., 1980. The scaling of vertical temperature spectra. Journal of Geophysical Research, 85:1917-1924.

Chriss, T. M. and Caldwell, D. R., 1979. The viscous sublayer on the Oregon shelf - scaling of sublayer thickness. EOS, 60:847.

Chriss, T. M. and Pak, H., 1977. Optical evidence of sediment resuspension - Oregon continental shelf. EOS, 58:410.

Dillon, T. M. and Caldwell, D. R., 1980. The Batchelor spectrum and dissipation in the upper ocean. Journal of Geophysical Research, 85:1910-1916.

Drake, D. E., 1974. Distribution and transport of suspended particulate matter in submarine canyons off southern California.

In: R. J. Gibbs (Editor), Suspended Solids in Water. Plenum, New York, pp. 133-154.

Dyer, A. J., 1974. Review of flux profile relationships. Boundary Layer Meteorology, 7:363-372.

Gordon, C. M., 1974. Intermittent momentum transport in a geophysical boundary layer. Nature, 248:392-394.

Harlett, J. C., 1972. Sediment transport on the northern Oregon Continental shelf. Ph.D. thesis, Oregon State University, Corvallis, 120 pp.

Heathershaw, A. D., 1974. "Bursting" phenomena in the sea. Nature, 248:394-395.

Heathershaw, A. D. and Simpson, J. H., 1948. The sampling variability of the Reynolds stress and its relation to boundary shear stress and drag coefficient measurements. Estuar. Coast. Mar. Sci., 6:263-274.

Jerlov, N. G., 1968. Optical Oceanography. Elsevier, Amsterdam, 194 pp.

Komar, P. D., Kulm, L. D. and Harlett, J. C., 1974. Observations and analysis of bottom turbid layers on the Oregon continental shelf. Journal of Geology, 82:105-111.

Kullenberg, G., 1974. Distribution of particulate matter in northwest African upwelling area. In: R. J. Gibbs (Editor), Suspended Solids in Water. Plenum, New York, pp. 195-202.

McCave, I. N., 1972. Transport and escape of fine-grained sediment from shelf areas. In: D. J. P. Swift, O. Pilkey and D. Duane (Editors), Shelf Sediment Transport: Process and Pattern.

Dowden, Hutchinson and Ross, Stroudsburg, PA, pp. 225-248.

Monin, A. S. and Yaglom, A. M., 1971. Statistical Fluid Mechanics. MIT Press, Cambridge, 769 pp.

Osborn, T. R. and Cox, C. S., 1972. Oceanic fine structure. Geophysical Fluid Dynamics, 3:320-345.

Pak, H. and Zaneveld, J. R. V., 1977. Bottom nepheloid layers and bottom mixed layers observed on the continental shelf off Oregon. Journal of Geophysical Research, 82:3921-3931.

Peterson, R. E., 1978. A study of suspended particulate matter: Arctic Ocean and Northern Oregon continental shelf. Ph.D. thesis, Oregon State University, Corvallis, 122 pp.

Runge, E. J., 1966. Continental shelf sediments, Columbia River to Cape Blanco, Oregon. Ph.D. thesis, Oregon State University, Corvallis, 143 pp.

Taylor, P. A. and Dyer, K. R., 1977. Theoretical models of flow near the bed and their implications for sediment transport. In: E. D. Goldberg, I. N. McCave, J. J. O'Brien and J. H. Steele (Editors), The Sea, Volume 6. Wiley, New York, pp. 579-609.

Tennekes, H. and Lumley, J. L., 1972. A First Course in Turbulence. MIT Press, Cambridge, 300 pp.

Zaneveld, J. R. V., 1973. Variation of optical sea parameters with depth. In: Optics of the Sea, lecture series No. 61, Agard, NATO, France.

TABLE 1
Friction velocities for shallow water stations

Sequence number	u_* (cm s^{-1})	$\bar{U}$ (cm s^{-1})	$u_*^2/\bar{U}^2$	$\frac{ku_*z}{2}$ $z = 100$ cm (cm ^{2} s^{-1})
78823A	0.45	20.0*		18.5
78921A	0.15	3.4*		6.2
78922A	0.04	1.6*		1.6
79611A+	0.41	9.6	1.8×10^{-3}	16.8
79612A	0.50	12.3	1.6×10^{-3}	20.5
79612C	0.19	9.4	0.4×10^{-3}	7.8
79612D+	0.34	6.7	2.6×10^{-3}	13.9
79612D'+	0.19	3.8	2.5×10^{-3}	7.8
79612E	0.16	6.2	0.7×10^{-3}	6.6
79613A+	0.22	3.9	3.2×10^{-3}	9.0
(mean)	(0.27)		(1.8×10^{-3})	(10.9)
(standard deviation)	(0.79)		(0.9×10^{-3})	(5.9)

+ Periods of steady mean current
* 1 hour average currents measured approximately 8 m above the bottom at 45°20.1'N, 124°08.8'W by Dr. Barbara Hickey of the University of Washington. Other current measurements were made 59 cm above the bottom.

TABLE 2
Friction velocities for deep water stations

Sequence number	u_* (cm s^{-1})	$\bar{U}$ (cm s^{-1})	$(u_*/\bar{U})^2$	ku_*z $z = 100$ cm (cm^2 s^{-1})	$\bar{K}$ (cm^2 s^{-1})
79419A	0.16	*		6.6	12 ‡
79420B	0.11	*		4.5	+
79421A	0.08	3.0	0.7×10^{-3}	3.3	1
79422A+	0.18	3.2	3.2×10^{-3}	7.4	3
79605A+	0.18	3.6	2.5×10^{-3}	7.4	6
79606A	0.23	*		9.0	3
79607A	0.24	2.8	7.3×10^{-3}	9.8	5 ‡
79607B	0.23	7.8	0.9×10^{-3}	9.4	+
(mean)	(0.18)		(2.9×10^{-3})	(7.2)	
(standard deviation)	(0.05)		(2.4×10^{-3})	(2.2)	

+ Periods of steady mean current
* Below threshold of current meter. All current measurements made 59 cm above bottom.
‡ Mean temperature gradient not resolved

TABLE 3
Models for the distribution of suspended sediment

Model	Assumptions	Predicted profile
I	Turbulent mixing K_s = constant	$C(z) = A - Jz/K_s$
II	Turbulent mixing $K_s = ku_*z$	$C(z) = A - (J/ku_*) \ln z$
III	Turbulent mixing and settling, K_s = constant	$C(z) = -J/w_s + Be^{-w_s z/K_s}$ $\ln(C + J/w_s) = \ln B - w_s z/K_s$
IV	Turbulent mixing and settling, $K_s = ku_*z$	$C(z) = -J/w_s + Bz^{-w_s/(ku_*)}$ $\ln(C + J/w_s) = \ln B - w_s/(ku_*)$

TABLE 4
Settling velocities (cm s^{-1}) from Model IV with several values of flux

Sequence	J/w_s ($\mu g \ell^{-1}$)	upward +150	upward +100	0	downward -100	downward -150
78823C		.004	.004	.005	.007	.009
79611A		.003	.004	.004	.006	.006
79612A		.002	.003	.003	.004	.005
79612C		.002	.002	.003	.004	.005
79612D		.003	.003	.004	.006	.007
79612D'		.002	.002	.003	.004	.004
79613A		.002	.002	.003	.004	.004

FIGURE CAPTIONS

FIGURE 1. Profiles of temperature (T), transmissivity (O) and Cox number. (a) August 1978, (b) September 1978, (c) April 1979 and (d) June 1979. The gap in the 1978 data at approximately 83 m was caused by a failure in the recording system.

FIGURE 2. Dissipation rate, ε, vs. distance above the sediment for profile 79612E2. The solid line is $u_* = 0.16$ cm s^{-1}.

FIGURE 3. Dissipation rate scaled by u_*^3 for the six steady mean current sequences. These values of u_* are obtained from the 59 cm current meter assuming a non dimensional viscous sublayer thickness of 11. The solid line is $(kz)^{-1}$.

FIGURE 4. Comparison of average particle concentration profile for sequence 79612C with model I (dashed line), models II and IV (solid line) and model III (dotted line). Model II and model IV with all values of flux differ less than 5 $\mu g \ell^{-1}$ for z > 30 cm.

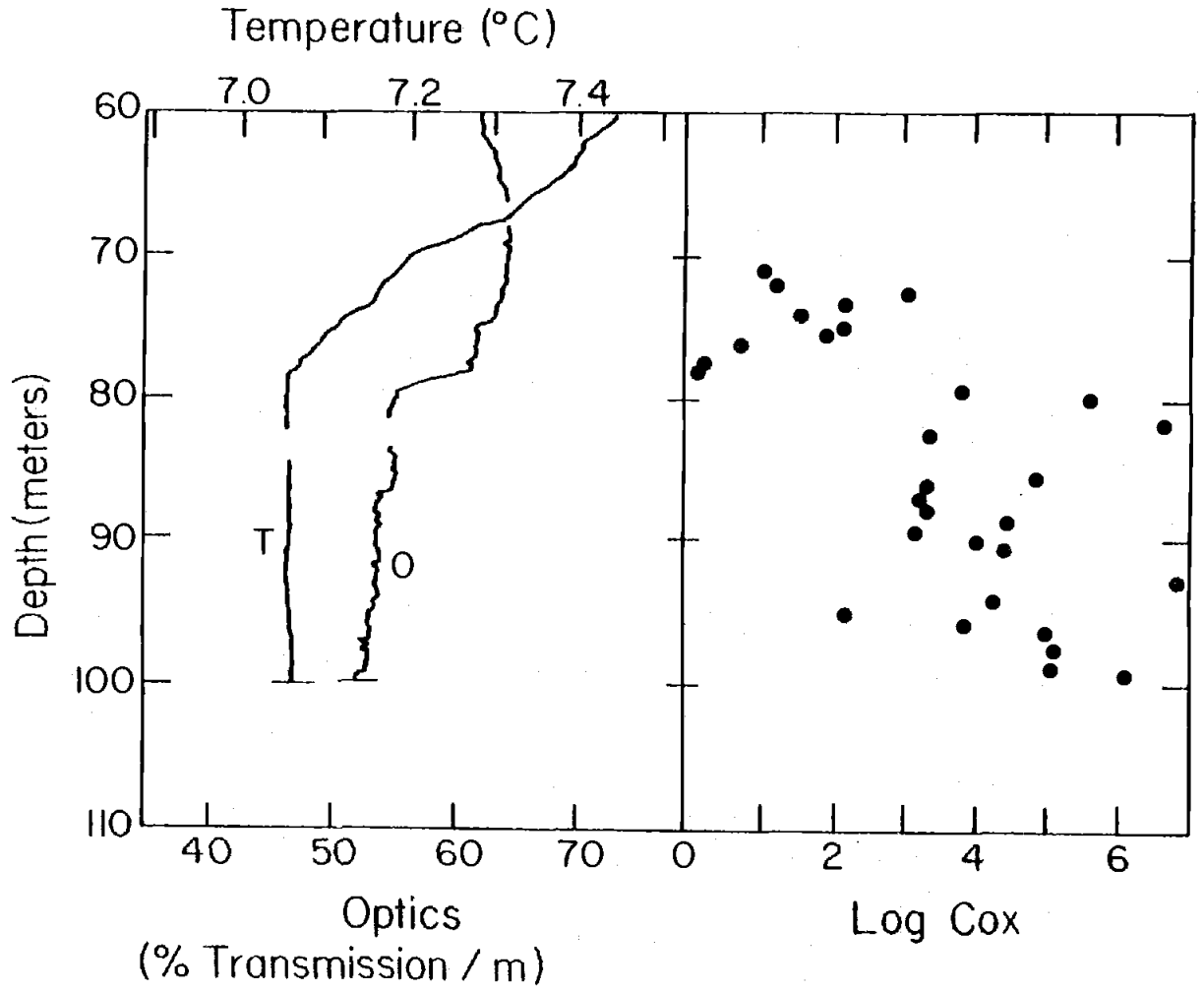
Temperature (°C)
7.0
7.2
7.4
60
70
80
90
100
110
Depth (meters)
T
O
40
50
60
70
Optics
(% Transmission / m)
0
2
4
6
Log Cox

Figure I-1a

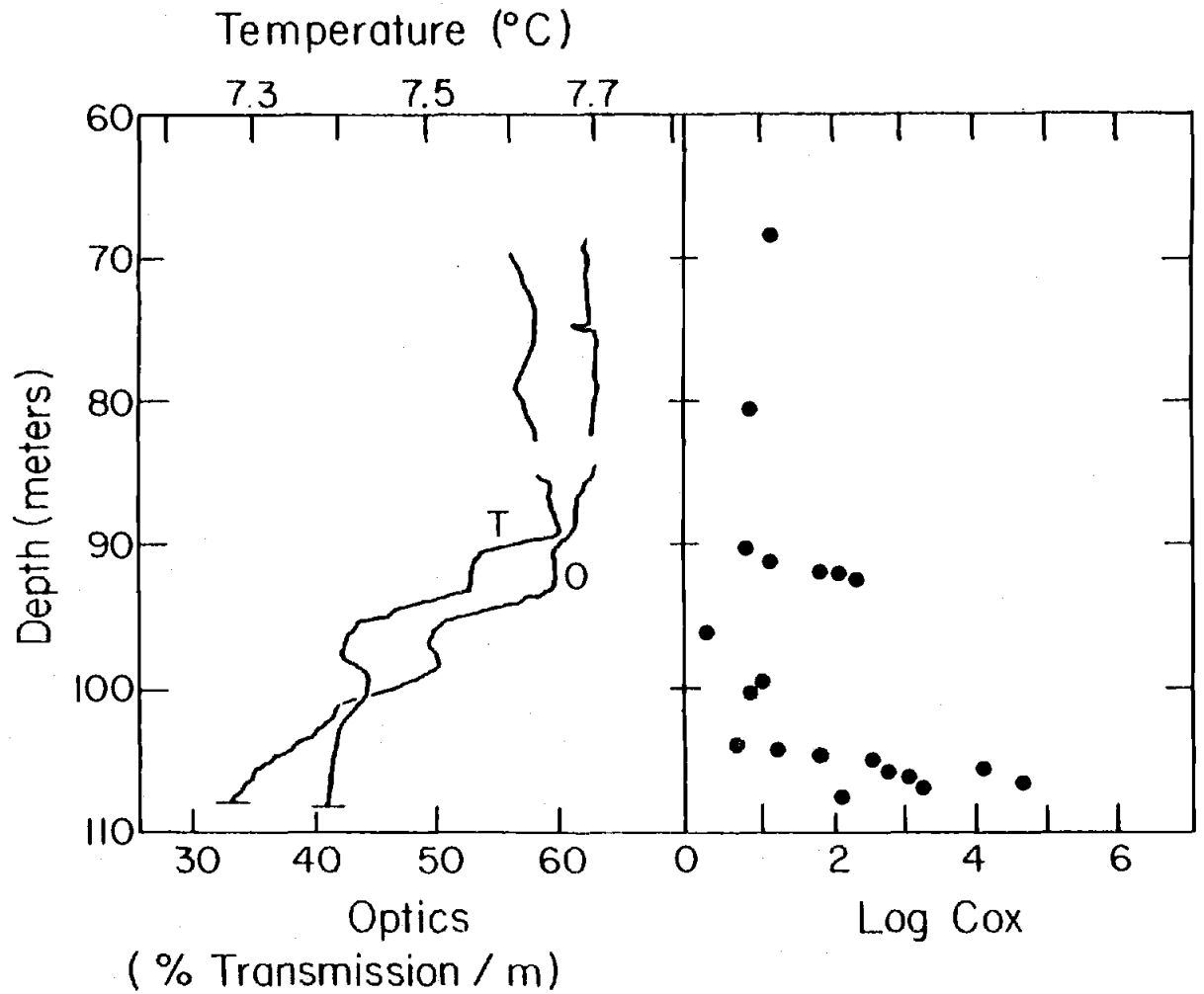
Temperature (°C)
7.3
7.5
7.7
60
70
80
90
100
110
Depth (meters)
T
O
30
40
50
60
Optics
(% Transmission / m)
0
2
4
6
Log Cox

Figure I-1b

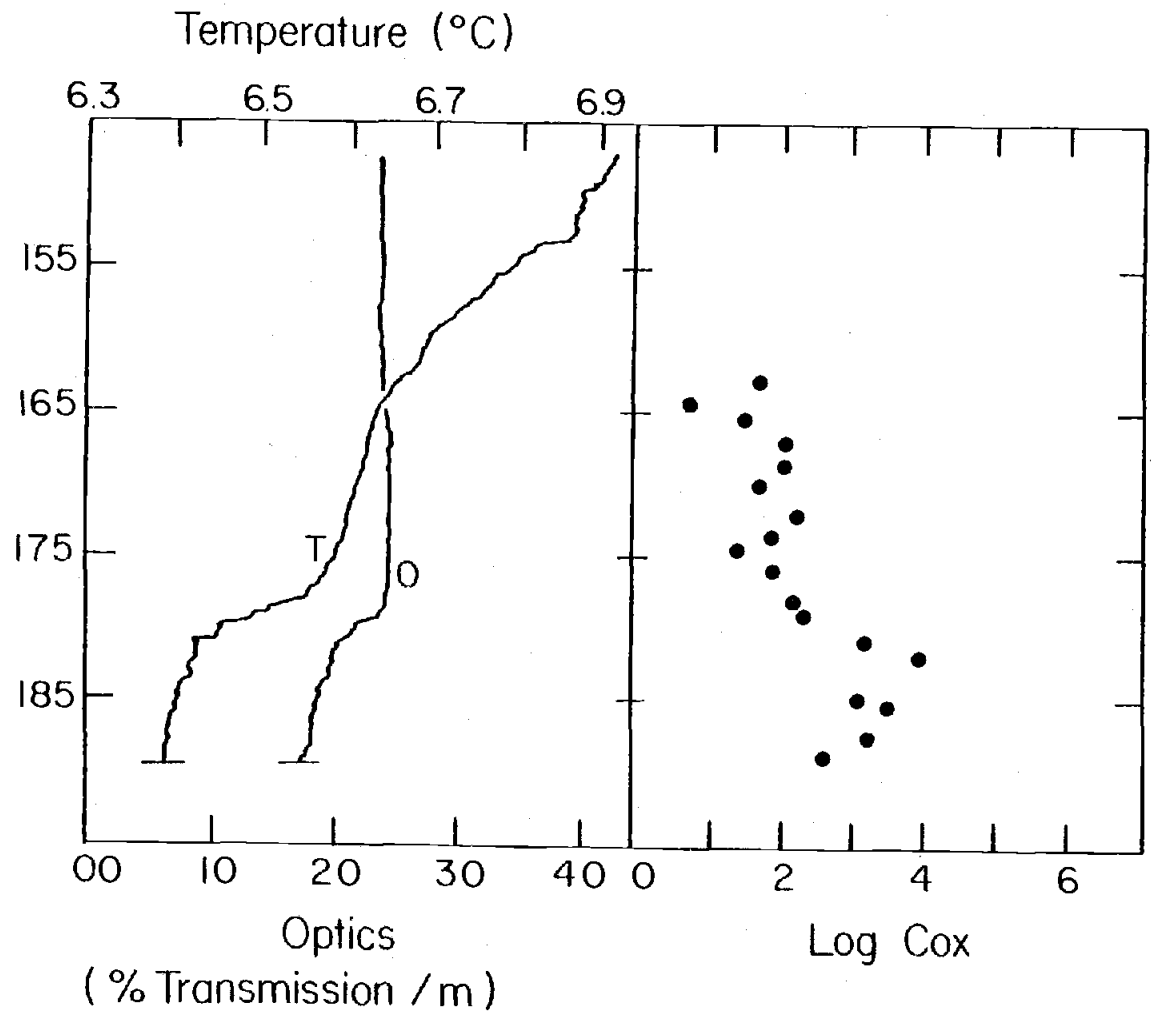
Temperature (°C)
6.3
6.5
6.7
6.9
155
165
175
185
T
O
00
10
20
30
40
Optics
(% Transmission / m)
0
2
4
6
Log Cox

Figure I-1c

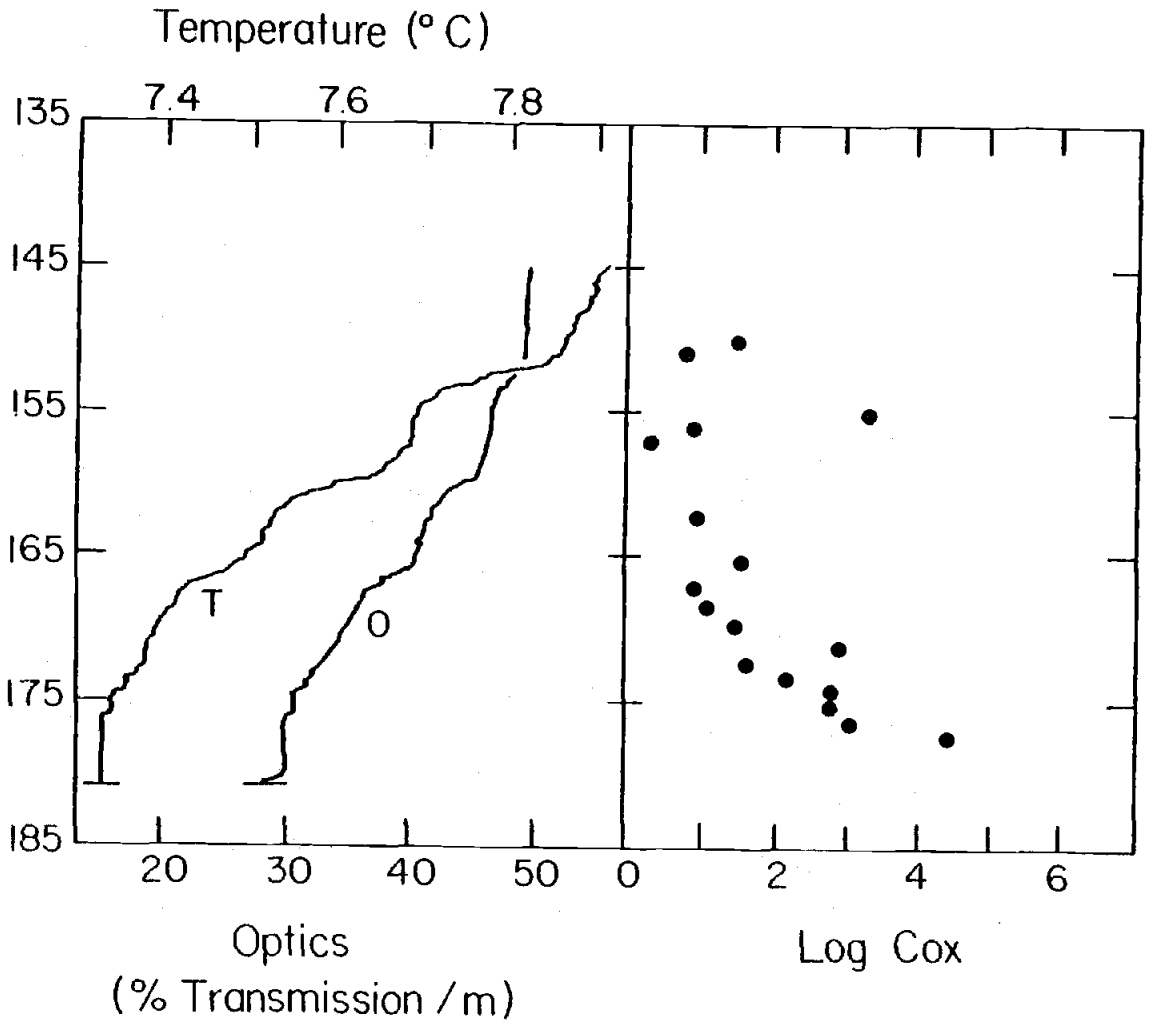
Temperature (° C)
7.4
7.6
7.8
135
145
155
165
175
185
T
O
20
30
40
50
0
2
4
6
Optics
(% Transmission / m)
Log Cox

Figure I-1d

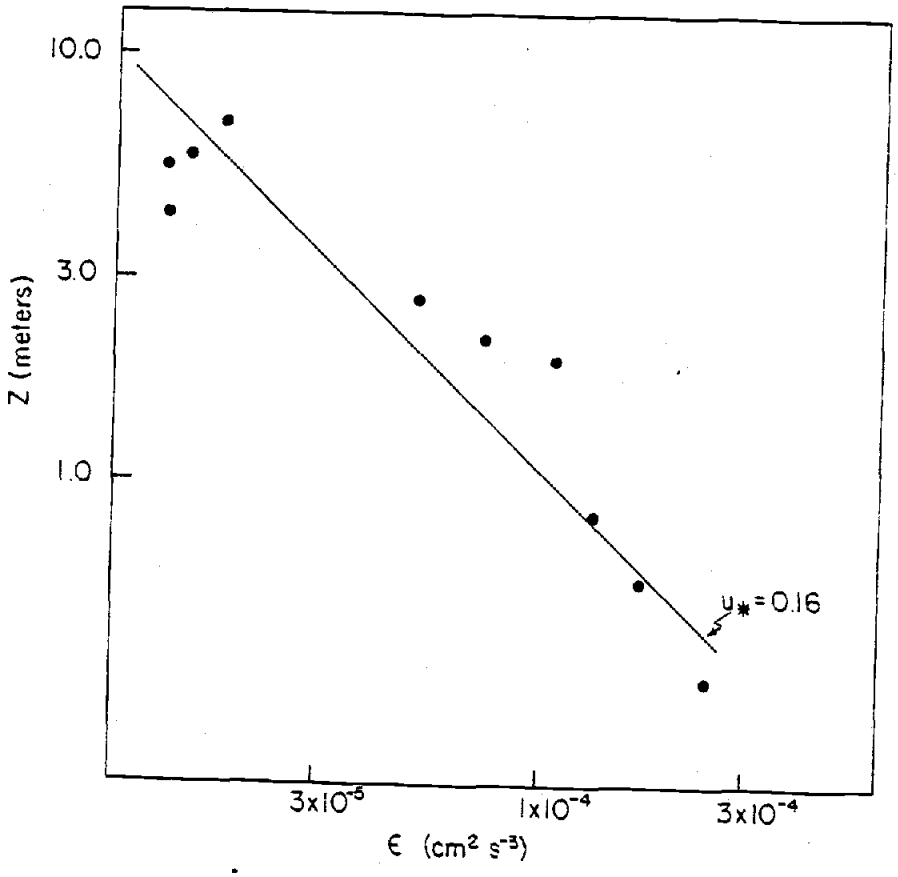
10.0
3.0
1.0
Z (meters)
$u_* = 0.16$
3×10^{-5}
1×10^{-4}
3×10^{-4}
ϵ (cm^2 s^{-3})

Figure I-2

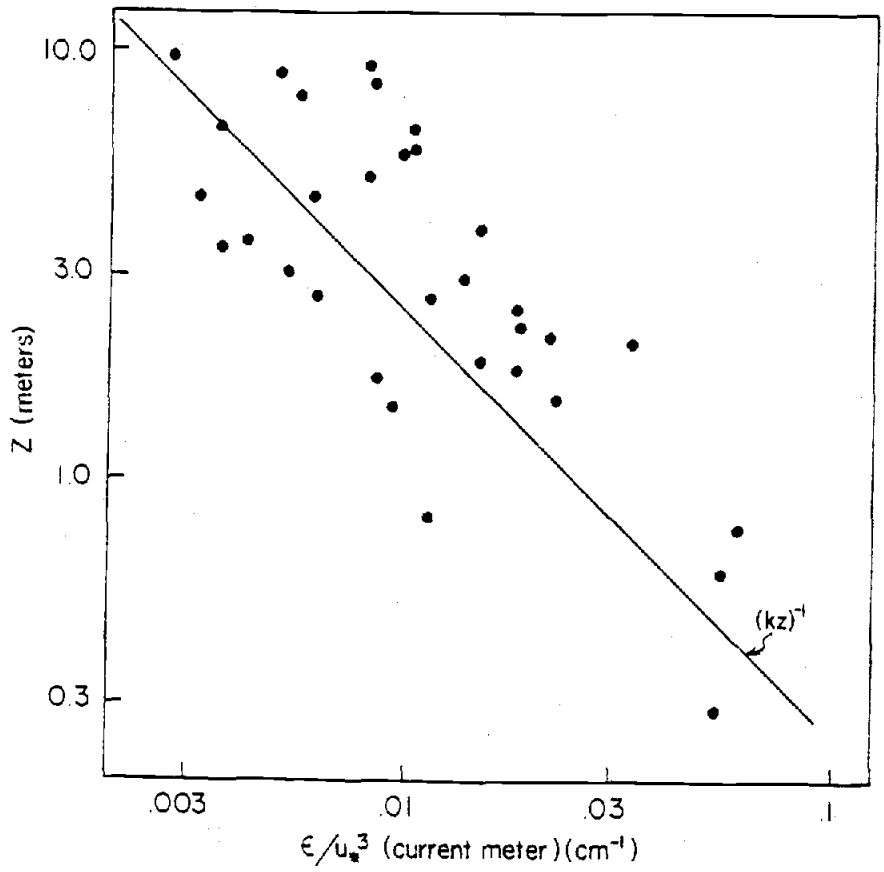
10.0
3.0
1.0
0.3
Z (meters)
.003
.01
.03
.1
ϵ/u_*^3 (current meter) (cm^{-1})
$(kz)^{-1}$

Figure I-3

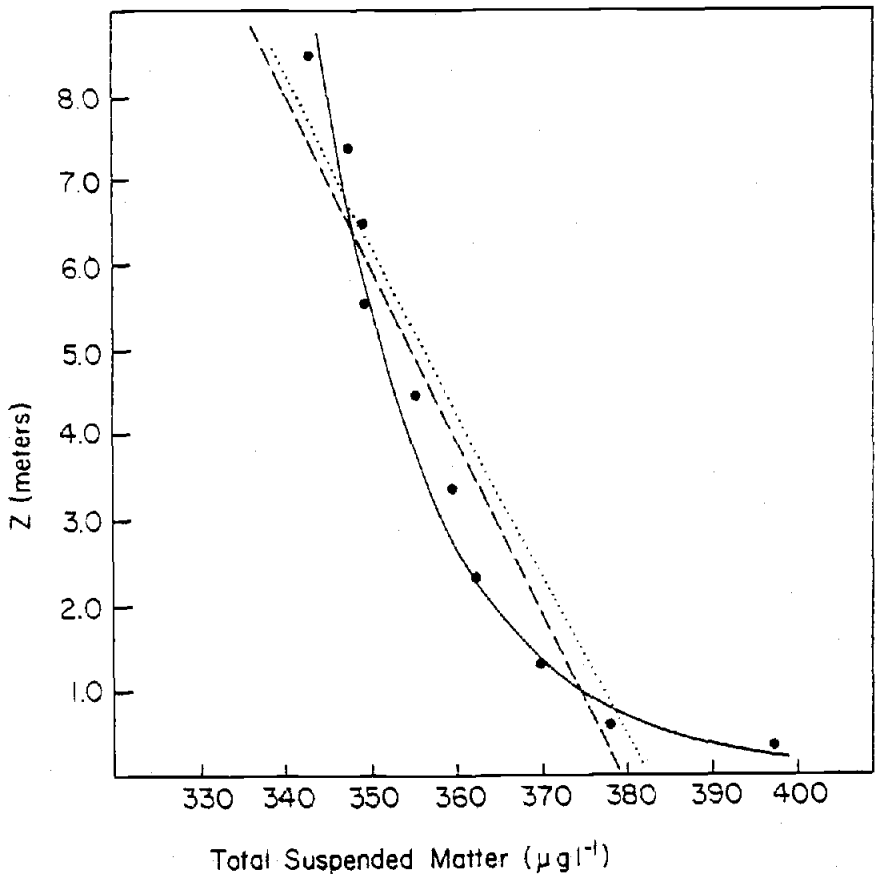
8.0
7.0
6.0
5.0
4.0
3.0
2.0
1.0
Z (meters)
330
340
350
360
370
380
390
400
Total Suspended Matter (μg l⁻¹)

Figure I-4

An Inertial Subrange in Microstructure Spectra

P. A. Newberger

School of Oceanography

Oregon State University

Corvallis, Oregon 97331

USA

July 1980

ABSTRACT

An inertial subrange was found in spectra calculated from vertical profiles of temperature gradient recorded in the bottom boundary layer of the Oregon shelf. Spectra were calculated for 53-cm vertical segments. An ensemble average of those spectra that were fully resolved and had high Cox number was compared to the universal form. Good agreement was found with the Batchelor form. The high wavenumber end of the inertial range was resolved. A relationship between the Kolmogorov constant for temperature, β, and the Batchelor constant, q, was established, $\beta q^{-2/3} = 0.172$ (± 0.012). If $\beta = 0.5$, as determined from atmospheric data, $q = 4.95$ ($4.28 < q < 6.65$) and the transition from the inertial to the viscous-convective range occurs at a wavenumber $k = 0.035\ k_K$ ($0.021 < k/k_K < 0.043$) where k_K is the Kolmogorov wavenumber.

INTRODUCTION

Kolmogorov (1941) proposed that the small-scale properties of turbulent fluids are universal when scaled by factors depending only on ε, the dissipation rate for kinetic energy, and ν, the kinematic viscosity, if the Reynolds number is sufficiently large. In this equilibrium range of wavenumbers, the eddies are statistically independent of the mechanism which generates the turbulence. If the Reynolds number is large enough, the equilibrium range will include an inertial subrange with length-scales large enough that viscosity is not important. Neither production nor dissipation of turbulent energy occurs in the eddies in this subrange.

Obukhoff (1949) and Corrsin (1951) independently assumed that Kolmogorov's hypotheses apply to the distribution of temperature in a turbulent fluid if the temperature variations are so small that buoyancy effects are not important. They each deduced the existence of an inertial-convective range where temperature variance is neither produced nor dissipated. In this range, statistical properties, such as the temperature spectrum, depend only on ε and χ, the dissipation rate of temperature variance.

Batchelor (1959) determined the form of the temperature spectrum for higher wavenumbers where viscous and diffusion effects are important. For fluids with large Prandtl number ($\nu >> D$, where D is the thermal diffusivity), such as water, the Batchelor spectrum contains two subranges, the viscous-convective, where viscosity is effective but thermal diffusivity is not, and the viscous-diffusive, where both are important.

A number of observations of temperature or temperature-gradient spectra have been made in the ocean (e.g. Grant et al., 1968; Gregg, 1976, 1977; Nasymth, 1970; Elliot and Oakey, 1976; Dillon and Caldwell, 1980a). These observations have, in general, two purposes: to determine whether turbulence theory applies to the ocean and to gain understanding of small-scale flow dynamics. Comparison with the predicted universal form has been unfavorable in several cases (Nasmyth, 1970; Elliot and Oakey, 1976). Dillon and Caldwell (1980a) found good agreement with the Batchelor spectrum in the surface mixed layer when the Cox number, $(\langle dT^2/dz\rangle/\langle dT/dz\rangle^2)$ is greater than 2500. They suggest that the broadening of the spectrum at lower Cox number is caused by contamination by fine structure.

The inertial subrange has not been identified in vertical temperature microstructure spectra. Batchelor (1959) suggests that the Batchelor form may be found even if the Reynolds number is not high enough for an inertial range to exist. One reason that the inertial range is not seen in vertical microstructure may be that the turbulence is seldom stationary over large enough vertical scales (Dillon and Caldwell, 1980a). Fine structure and internal waves may also contaminate the spectrum (Gregg, 1977).

An attempt to determine whether the inertial subrange ever exists in the ocean must take these difficulties into account. Observations should be made in a region of small stratification so that the vertical component of the turbulence is not suppressed. High Cox numbers and a lack of fine structure will prevent contam-

ination of the spectrum. The bottom layer on the Oregon shelf satisfies these conditions (Caldwell, 1976, 1978; Newberger and Caldwell, 1980). Furthermore, the spectral cutoff (defined to be the wavenumber at which the temperature-gradient spectrum falls to 10% of its maximum) often occurs at very high wavenumber so that part of the inertial range, if it exists, will be reached in spectra from regions of small vertical extent.

THE DATA

Sixteen vertical profiles (Fig. 1) of temperature and temperature gradient were made in a 2.5 hour period in 85 m of water on the Oregon shelf (45°N) on October 22, 1977. The profiles were made with one freely-falling microstructure instrument and during the sampling period no changes were made affecting the descent rate of the instrument. This instrument responds quickly to changes in the vertical velocity of the water (Dillon and Caldwell, 1980b) so that the speed of the instrument through the water (9.1 cm s^{-1}) did not change during the sampling period.

Temperature-gradient spectra, corrected for thermistor response (Dillon and Caldwell, 1980a), were calculated for each 53 cm segment (512 points) of the bottom layer for each of these profiles. Of these segments, 77 were chosen for this analysis. There were three factors determining which segments were chosen. First, the Cox number for each chosen segment is large (>2000) (Dillon and Caldwell, 1980a). Second, the cutoff wavenumber (the wavenumber at which the spectrum falls to 10% of its maximum value) lies within

the range of resolved wavenumbers. Finally the spectrum was required to be clearly above the level of instrumental noise.

Taylor's hypothesis is required to express vertical microstructure spectra in terms of wavenumber. Lumley (1965) has shown that violations of this hypothesis caused by large turbulent intensities can cause distortion of the high wavenumber spectrum. The distortion depends on the relative magnitude of the typical turbulent velocity fluctuation, u', and the advection velocity, here the instrument descent rate, 9.1 cm s^{-1}. The mean current, measured by a nearby current meter, varied from 10 to 19 cm s^{-1} during this experiment. Using the usual estimate for the friction velocity, u_* ($u_* = \bar{U}/30$), u_* is at most 0.7 cm s^{-1}. In the bottom layer u' and u_* are comparable and Lumley's analysis indicates that with u' of this magnitude, distortion due to this effect is negligible.

THEORETICAL BACKGROUND

The one-dimensional Batchelor spectrum for the temperature gradient can be written as (Gibson and Schwarz, 1963)

$$S(k) = \pi^{1/2}\, q^{1/2}\, \chi\, k_B^{-1}\, D^{-1}\, f((2q)^{1/2}\, k\, k_B^{-1}) \qquad (1)$$

where q is a universal constant, k_B the Batchelor wavenumber ($k_B = (\varepsilon \nu^{-1} D^{-2})^{1/4}$), ε the dissipation rate for kinetic energy, ν the kinematic viscosity, D the thermal diffusivity and χ the dissipation rate for temperature variance satisfying

$$\chi = 6D \int_0^\infty S(k)dk = 6D\overline{(\frac{dT}{dz})^2}. \qquad (2)$$

The universal function f is given by

$$f(\zeta) = (2\pi)^{-1/2}\,\zeta(\exp(-1/2\,\zeta^2) - \zeta\int_{\zeta}^{\infty}\exp(-1/2\,y^2)dy). \qquad (3)$$

The transition from the inertial to the viscous-convective range occurs at wavenumber $k_* = C_*\,Pr^{-1/2}\,k_B = C_*\,k_K$ where k_K is the Kolmogorov wavenumber ($k_K = (\varepsilon\nu^{-3})^{1/4}$), Pr is the Prandtl number ($Pr = \nu/D$) and C_* is a universal constant. For wavenumbers in the inertial range

$$S(k) = \beta\chi\varepsilon^{-1/3}\,k^{1/3} \qquad (4)$$

where β is also universal. The three constants, β, q and C_* are related by the requirement that the spectrum be continuous at k_*, so that there are two independent constants that must be determined to describe the predicted spectrum.

Caldwell et al. (1980) have shown that for vertical temperature gradient spectra the cutoff wavenumber is related to the Batchelor wavenumber. For the Batchelor spectrum, the relationship depends only on the universal constant q. Numerical evaluation of (3) shows that the universal function f falls to 10% of its maximum when the arguement ζ is equal to 2.225. This implies that the cutoff occurs at $k = \alpha k_B$ where $\alpha = 2.225(2q)^{-1/2}$. This relationship can be used to define a scaling wavenumber $k_s = \alpha k_K = \alpha Pr^{-1/2}\,k_B$.

The spectrum is then non-dimensionalized by multiplying (3) and (4) by $(k_s\nu\chi^{-1})$:

$$S(k)\{k_s\nu\chi^{-1}\} = \alpha(\pi q Pr)^{1/2}\,f((2q)^{1/2}\,Pr^{-1/2}\,\alpha\kappa), \quad \kappa_* \leq \kappa \qquad (5)$$

$$S(k)\{k_s\nu\chi^{-1}\} = \alpha^{4/3}\,\beta\kappa^{1/3}, \quad \kappa_o < \kappa \leq \kappa_* \qquad (6)$$

where $\kappa = k/k_s$ is the non-dimensional wavenumber, $\kappa_* = k_*/k_s$ and κ_o is the low wavenumber end of the inertial range. In this form (Fig. 2) the spectrum above κ_* is independent of all parameters except the Prandtl number ($\alpha q^{1/2}$ is constant), but values in the inertial range depend on both q and β.

There have been various attempts to evaluate the universal constants β, q and C_*. The Kolmogorov constant β is best known. Williams and Paulson (1977) found $\beta \approx 0.5$ from atmospheric measurements. Paquin and Pond (1971) found $\beta \approx 0.4$ also in the atmosphere. Grant et al. (1968) found $\beta = 0.31$ in the ocean, while Gibson and Schwarz (1963) found $\beta = 0.35 \pm 0.05$ (standard deviation) in the laboratory.

Grant et al. (1968) estimated $q = 3.9 \pm 1.5$ and $C_* = 0.024 \pm 0.008$ (standard error estimates), Gibson (1968) suggested on theoretical grounds that $3^{1/2} < q < 2(3)^{1/2}$. Gibson et al. (1970) found C_* to be 0.03 and 0.04.

THE SCALED SPECTRUM

If the universal scaling is appropriate to the spectra from the bottom layer, the non-dimensionalized spectra should collapse to the form of Figure 1. Although there is considerable scatter at the low wavenumber end where each point represents a single spectral estimate (Fig. 3), good agreement with the universal form is revealed when the spectra are ensemble-averaged (Fig. 4). The three lowest wavenumbers do appear to lie in the inertial subrange. The values of the averaged spectrum at the inertial-range points to-

gether with equation (6) imply that $\beta\alpha^{4/3} = 0.318$ (standard deviation of the mean 0.020). This is equivalent to $\beta q^{-2/3} = 0.172$ (standard deviation of the mean 0.012). Limits can be placed on these estimates by considering the largest and smallest values of $\beta\alpha^{4/3}$ such that equation (6) lies within the standard error of the mean for each of the inertial-range points. Thus $0.256 < \beta\alpha^{4/3} < 0.347$ and $0.140 < \beta q^{-2/3} < 0.190$. The wavenumber for transition from the inertial range can be determined from the intersection of equations 5 and 6 with $\beta\alpha^{4/3} = 0.318$ and occurs at $\kappa_* = 0.049$ ($0.035 < \kappa_* < 0.057$). An independent estimate of ε, from velocity spectra for example, would be required to evaluate the constants separately.

Atmospheric data are more extensive and probably more accurate than oceanic measurements. In the inertial range, the difference in viscosity of air and water is not important. Therefore we assume $\beta = 0.5$ (Williams and Paulson, 1977) to determine q and C_*. We find that $q = 4.95$ ($6.65 > q > 4.28$) and $C_* = 0.035$ ($0.021 < C_* < 0.043$). If in fact $\beta = 0.31$ (Grant et al., 1968), the lowest estimate of β, $q = 2.42$ and $C_* = 0.047$. Experimental evidence tends to support the lower value of C_*.

CONCLUSIONS

The inertial subrange is observed in temperature-gradient spectra from microstructure data recorded in the bottom layer on the Oregon shelf. Good agreement is found for higher wavenumbers between the ensemble averaged spectrum and the Batchelor form. A

relationship between the universal constants β and q, $\beta q^{-2/3} = 0.172$, is established. If $\beta = 0.5$, as indicated by atmospheric measurements, $q = 4.95$ and $C_* = 0.035$. These observations were made under conditions nearly ideal for the existence of fully developed turbulence. In this case the inertial range exists, but such favorable conditions may be uncommon in the ocean.

ACKNOWLEDGEMENTS

This research was supported by NSF Grant OCE77-20242 and OCE79-18904.

REFERENCES

Batchelor, G. K., Small-scale variation of convected quantities like temperature in turbulent fluid, Journal of Fluid Mechanics, 5,113-133, 1959.

Caldwell, D. R., Fine-scale temperature structure in the bottom mixed-layer on the Oregon shelf, Deep-Sea Research, 23,1025-1036, 1976.

Caldwell, D. R., Variability of the bottom mixed layer on the Oregon shelf, Deep-Sea Research, 25,1235-1243, 1978.

Caldwell, D. R., T. M. Dillon, J. M. Brubaker, P. A. Newberger and C. A. Paulson, The scaling of vertical temperature gradient spectra, Journal of Geophysical Research, 85,1917-1924, 1980.

Corrsin, S., On the spectrum of isotropic temperature fluctuations in an isotropic turbulence, Journal of Applied Physics, 22,469-473, 1951.

Dillon, T. M. and D. R. Caldwell, The Batchelor spectrum and dissipation in the upper ocean, Journal of Geophysical Research, 85,1910-1916, 1980a.

Dillon, T. M. and D. R. Caldwell, High frequency internal waves at ocean station P, Journal of Geophysical Research, 85,3277-3284, 1980b.

Elliot, J. A. and N. S. Oakey, Spectrum of small-scale oceanic temperature gradients, J. Fish. Res. Bd. Can., 33,2296-2306, 1976.

Gibson, C. H., Finestructure of scalar fields mixed by turbulence, 1,2, Physics of Fluids, 11,2305-2327, 1968.

Gibson, C. H. and W. H. Scharz, The universal equilibrium spectra of turbulent velocity and scalar fields, Journal of Fluid Mechanics, 16,365-384, 1963.

Gibson, C. H., R. R. Lyon, and I. Hirschsohn, Reaction product fluctuations in a sphere wake, AIAA J., 8,1859-1863, 1970.

Grant, H. L., B. A. Hughes, N. M. Vogel, and A. Moilliet, The spectrum of temperature fluctuations in turbulent flow, Journal of Fluid Mechanics, 34,423-442, 1968.

Gregg, M. C., Finestructure and microstructure observations during the passage of a mild storm, Journal of Physical Oceanography, 6,528-555, 1976.

Gregg, M. C., Variations in the intensity of small-scale mixing in the main thermocline, Journal of Physical Oceanography, 7,436-454, 1977.

Lumley, J. L., Interpretation of time spectra measured in high-intensity shear flows, Phys. Fluids, 8,1056-1062, 1965.

Nasmyth, P. W., Oceanic turbulence, Ph.D. thesis, 69 pp., Institute of Oceanography, Univ. of B.C., Vancouver, 1970.

Newberger, P. A. and D. R. Caldwell, Mixing and the Bottom Nepheloid Layer, Marine Geology, in press.

Obukhoff, A. M., Structure of the temperature field in turbulent streams, Buil. Acad. Sci. U.S.S.R., Geogr. Geophys. Sci., 13,58-69, 1949.

Paquin, J. E. and S. Pond, The determination of the Kolmogorov constants for velocity, temperature and humidity fluctuations from second- and third-order structure functions, Journal of

Fluid Mechanics, 50,257-269, 1971.

Williams, R. M. and C. A. Paulson, Microscale temperature and velocity spectra in the atmosspheric boundary layer, Journal of Fluid Mechanics, 83,547-567, 1977.

Figure Captions

Figure 1. A typical temperature profile. The solid lines indicate the 53 cm segments from which spectra were selected for this particular profile.

Figure 2. The theoretical scaled spectrum for

a) $\beta\alpha^{4/3} = 0.576$ ($\beta = 0.5$, $q = 2.0$)

b) $\beta\alpha^{4/3} = 0.318$ ($\beta = 0.5$, $q = 4.95$)

c) $\beta\alpha^{4/3} = 0.248$ ($\beta = 0.31$, $q = 2(3)^{1/2}$)

Figure 3. The seventy-seven non-dimensionalized spectra.

Figure 4. The ensemble averaged spectrum. The bars represent the standard error of the mean; the solid line is the Batchelor spectrum.

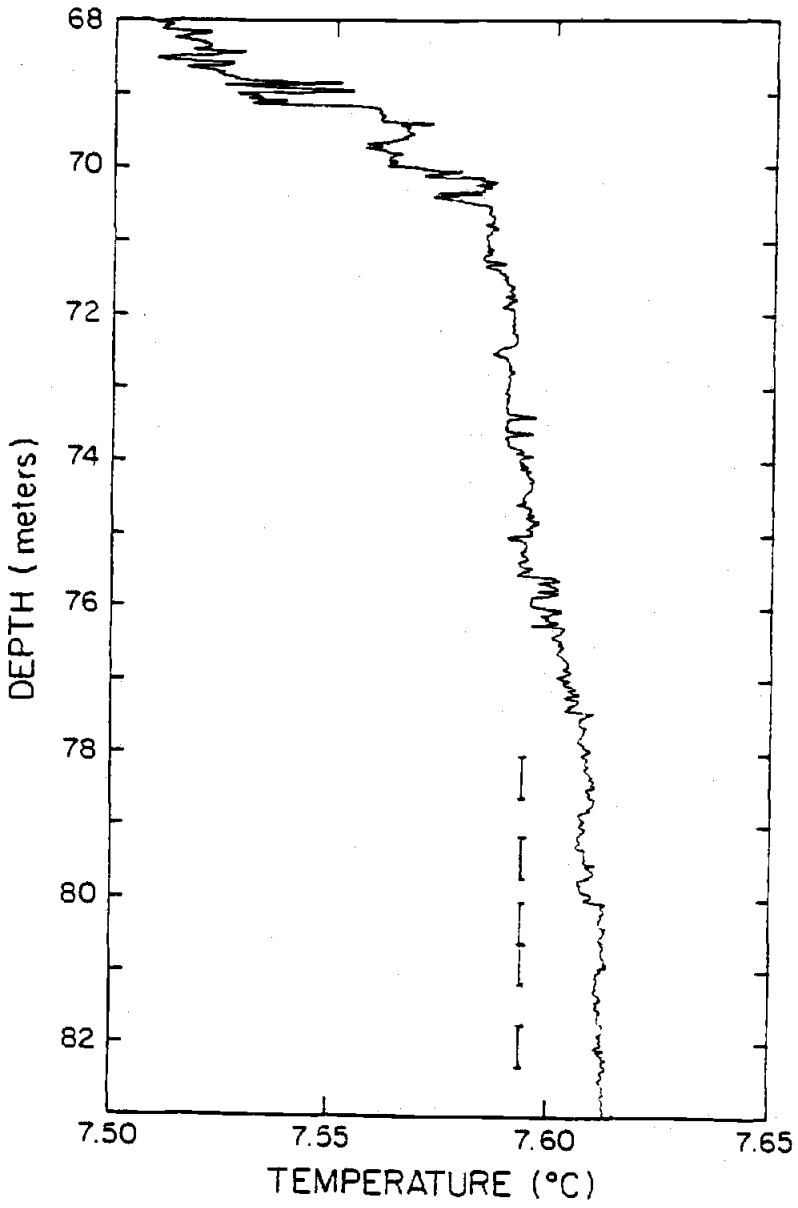
68
70
72
74
76
78
80
82
DEPTH (meters)
7.50
7.55
7.60
7.65
TEMPERATURE (°C)

Figure II-1

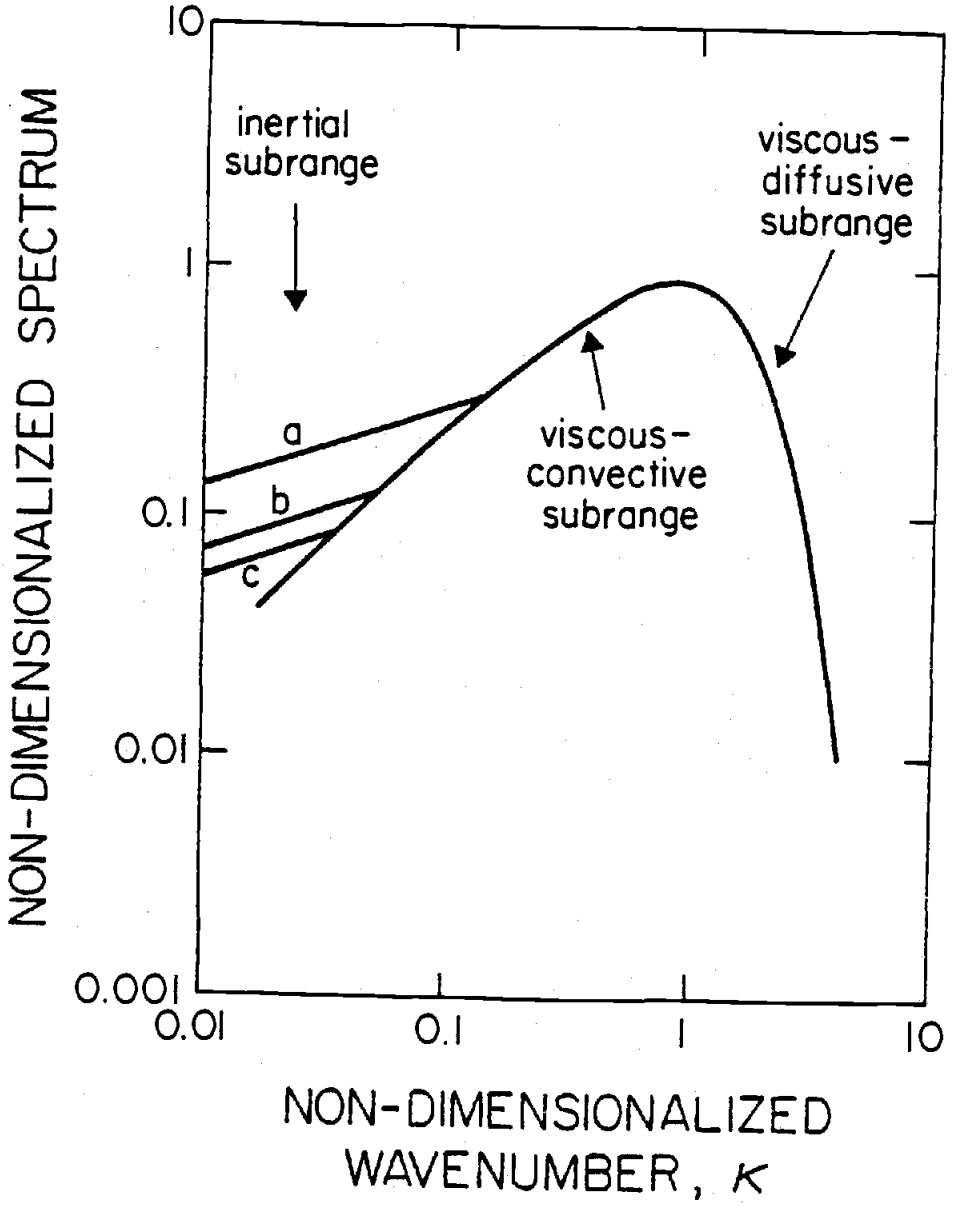
10
1
0.1
0.01
0.001
0.01
0.1
1
10
NON-DIMENSIONALIZED SPECTRUM
NON-DIMENSIONALIZED WAVENUMBER, κ
inertial subrange
viscous - diffusive subrange
viscous - convective subrange
a
b
c

Figure II-2

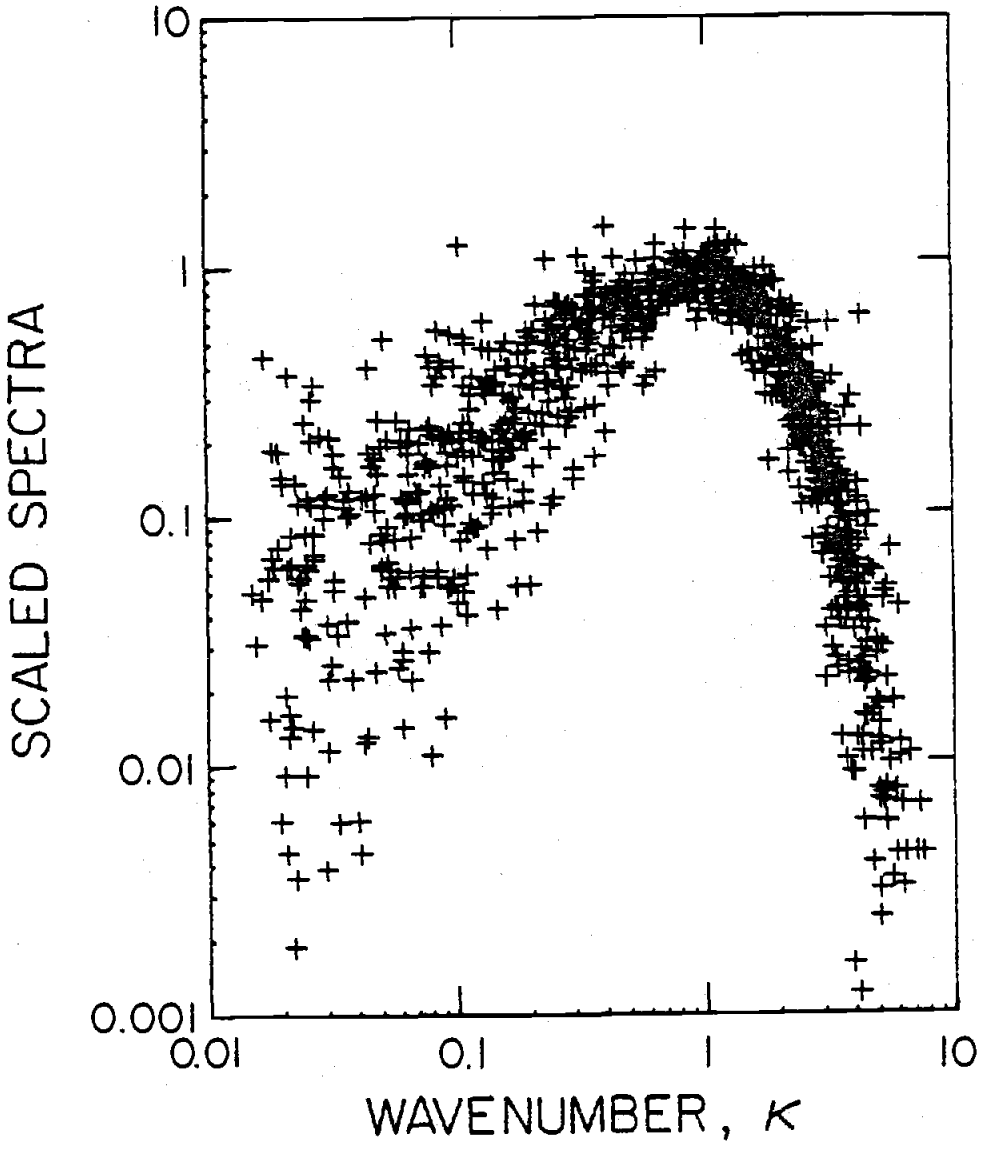

Figure II-3

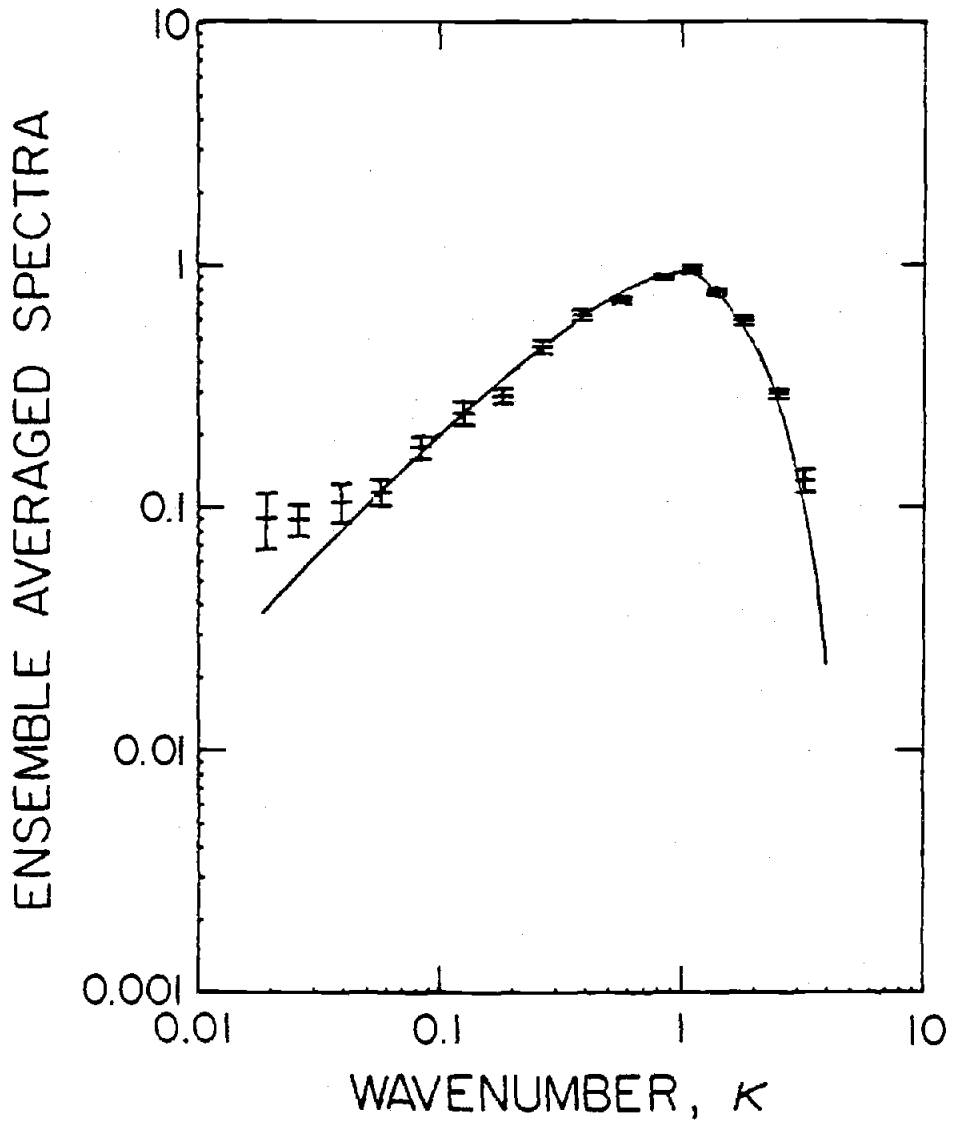
ENSEMBLE AVERAGED SPECTRA
10
1
0.1
0.01
0.001
0.01
0.1
1
10
WAVENUMBER, κ

Figure II-4